

## $p - air$ production cross-section and uncorrelated mini-jets processes in $pp$ -scattering

Daniel A. Fagundes<sup>1,a</sup>, Agnes Grau<sup>2,b</sup>, Giulia Pancheri<sup>3,c</sup>, Yogendra N. Srivastava<sup>4,d</sup>, and Olga Shekhovtsova<sup>5,e</sup>

<sup>1</sup>Instituto de Física Teórica, UNESP, Rua Dr. Bento T. Ferraz, 271, Bloco II, 01140-070, São Paulo - SP, Brazil

<sup>2</sup>Departamento de Física Teórica y del Cosmos, Universidad de Granada, 18071 Granada, Spain

<sup>3</sup>INFN Frascati National Laboratories, Via E. Fermi 40, Frascati I00044, Italy

<sup>4</sup>Physics Department, University of Perugia, Perugia, Italy

<sup>5</sup>Kharkov Institute of Physics and Technology 61108, Akademicheskaya, 1, Kharkov, Ukraine  
Institute of Nuclear Physics PAN ul. Radzikowskiego 152 31-342 Krakow, Poland

**Abstract.** For the  $p - air$  production cross-section, we use a Glauber formalism which inputs the  $pp$  inelastic cross-section from a mini-jet model embedded in a single-channel eikonal expression, that provides the needed contribution of uncorrelated processes. It is then shown that current LO parton density functions for the  $pp$  mini-jet cross-sections, with a rise tempered by acollinearity induced by soft gluon re-summation, are well suited to reproduce recent cosmic ray results. By comparing results for GRV, MRST72 and MSTW parametrizations, we estimate the uncertainty related to the low- $x$  behavior of these densities.

### 1 Introduction

In this contribution we address the problem of how to relate accelerator data for  $proton - proton$  scattering to  $p - air$  production cross-section measurements from cosmic rays. This is a very old question [1, 2] and very ingenious ways to do so have been developed through the years [3]. The issue is often obfuscated by the need to estimate the contribution from elastic and diffractive processes, both in  $p - air$ , but mostly in  $pp$  collisions.

The question of whether it is  $\sigma_{total}^{pp}$  or  $\sigma_{inel}^{pp}$  which is input to the Glauber formalism was discussed in the context of heavy ion collisions in [4] and in high energy cosmic rays in [5]. Presently, most current analyses define a  $\sigma_{prod}^{p-air}$  through the inelastic cross-section, and a  $\sigma_{inel}^{p-air}$  through the total  $pp$  cross-section. In either case, elastic and quasi-elastic contributions need to be subtracted and a degree of uncertainty can arise from their parametrization. The definition of inelastic cross-section is also affected by uncertainties, both theoretically and experimentally, as seen in LHC experiments with different cuts in the forward region [6].

Here we shall show that the total  $p - air$  production cross-section can be obtained in a very direct way through the inelastic  $pp$  cross-section resulting from single-channel eikonal models. This formalism for the inelastic cross-section provides a description of non-

correlated inelastic processes [7], and thus avoids the problem of how to model diffraction and elastic cross-section. The description of the latter, including the elastic differential cross-section, is still not resolved, and is obtained through various parametrizations. A recent suggestion by the Telaviv group [8] has made efforts in this direction. Here we shall follow a different path.

It is important to stress that in the case of cosmic rays, first and foremost one needs an eikonal function which gives a description of the total  $pp$  cross-section, through a good understanding of the underlying physics. In this paper we describe  $proton - air$  production cross-section up to the recent AUGER measurement [9], using the inelastic  $pp$  cross-section obtained from a QCD mini-jet model with soft gluon re-summation [10, 11].

We have long advocated QCD mini-jets as the driving mechanism for the rise of all total cross-sections [12] and have proposed a mechanism based on infrared gluon resummation to tame the excessive rise with energy of the mini-jet cross-sections [13]. While the mini-jet cross-sections are seen to rise like a power law in energy, the proposed soft gluon resummation ansatz introduces a cut-off at large impact parameter values and brings the total cross-section close to a saturation of the Froissart bound. Thus, the emphasis of the present work is two fold. First to provide a good phenomenological description of cosmic  $p - air$  production cross-sections through a successful well accepted formalism, such as in the Glauber theory [1]. The second is to reconfirm that the rise of all total, elastic and inelastic cross-sections of protons on protons, or protons on nuclei and other hadrons, have the same origin: a rising

<sup>a</sup>e-mail: dfagundes@ift.unesp.br

<sup>b</sup>e-mail: igrau@ugr.es

<sup>c</sup>e-mail: giulia.pancheri@lnf.infn.it

<sup>d</sup>e-mail: yogendra.srivastava@gmail.com

<sup>e</sup>e-mail: olga.shekhovtsova@ifj.edu.pl

contribution from the increasing number (with energy) of low- $x$  gluons excited in the collision [14].

Since the '80s, many models have used mini-jets in total cross-section physics [15–17] and more recently in [18]. In most cases, the parton density functions [PDFs] are chosen or parametrized *ad hoc*. However, we believe that mini-jets can give interesting information only if used in connection with current LO parton densities, such as available through updated PDF libraries. As in any perturbative QCD calculation, this LO effect needs then to be complemented by other QCD effects, such as that of very soft gluons arising from the QCD confinement potential [13].

In this contribution, the focus is on reproducing the very high energy cosmic ray phenomena, as measured by the AUGER collaboration and beyond. At such energies, the proton can penetrate the nucleus and interact independently with each nucleon, in addition QCD effects, obfuscated at lower energies by screening effects, are now important. We shall use the simplest version of the Glauber model [19], with the following basic hypothesis when the target is a nucleus: i) for low transverse momentum collisions  $p_t \lesssim (1 \div 2) \text{ GeV}$ , the incoming proton does not penetrate the air nucleus and basically scatters off the surface, whereas, as the transverse momentum increases, the proton penetrates the nucleus of atomic number  $A$  and scatters off all the protons in the volume occupied by the nucleus. Thus the nuclear density seen by the incoming protons will only be proportional to  $A^{2/3}$  for the soft collisions, and to  $A$  for the hard part. (ii) For interactions with transverse momenta  $p_t \gtrsim (1 \div 2) \text{ GeV}$ , we shall employ QCD effects in the form of mini-jets and soft gluon emission as in the model developed in [10, 11, 13].

Neglecting momentarily the above surface/volume effect, we begin with the usual Glauber expression for the production cross-section in the impact parameter representation, as given by

$$\sigma_{prod}^{p-air}(E_{lab}) = \int d^2\mathbf{b}[1 - e^{-n_{p-air}(b,s)}] \quad (1)$$

with

$$n_{p-air}(b, s) = T_N(\mathbf{b})\sigma_{inel}^{pp}(s) \quad (2)$$

wherein  $T_N(\mathbf{b})$  is the nuclear density, for which we start by choosing a standard gaussian distribution,

$$T_N(b) = \frac{A}{\pi R_N^2} e^{-b^2/R_N^2}, \quad (3)$$

properly normalized to

$$\int d^2\mathbf{b} T_N(b) = A. \quad (4)$$

The parameters used in the profile (3), namely the average mass number of an ‘‘air’’ nucleus,  $A$ , and the nuclear radius,  $R_N$ , are the following:

$$A = 14.5, \quad R_N = (1.1 \text{ fermi})A^{1/3}. \quad (5)$$

The inelastic  $pp$  cross-section,  $\sigma_{inel}^{pp}$ , is obtained from  $pp$  scattering, with

$$\sigma_{inel}^{pp} = \int d^2\mathbf{b}[1 - e^{-2\chi_I(b,s)}] \quad (6)$$

$$\sigma_{tot}^{pp} = 2 \int d^2\mathbf{b}[1 - \Re e(e^{i\chi(b,s)})] \quad (7)$$

where  $\chi_I(b, s) = \Im m\chi(b, s)$  is the imaginary part of the eikonal function that defines the elastic amplitude. At high energy, it is a good approximation to neglect a possible real part of the eikonal function in Eq. (7) and write

$$\sigma_{tot}^{pp} = 2 \int d^2\mathbf{b}[1 - e^{-\chi_I(b,s)}] \quad (8)$$

This formalism gives both the total and the inelastic non-correlated cross-section, once the quantity  $\chi_I(b, s)$  is known. The latter is an important point in the discussion of  $p - air$  processes. The single-channel eikonal formalism for the inelastic cross-section given by Eq. (6) includes only non-correlated, Poisson distributed independent collisions. This can be seen easily by comparing this equation with a sum over all independent Poisson like distributions, as discussed in [7]. Thus the above single-channel eikonal has the virtue of identifying all non-correlated processes, which we argue (and later verify phenomenologically) are all the non-diffractive processes contributing to the  $p - air$  production cross-section. We notice here that this property of the single-channel eikonal is a hindrance when one wants to separate the purely elastic from the diffractive part, but it is exactly what one needs for  $p$ -air shower initiated measurements. We shall return to this point again later.

In the following, we shall first consider  $pp$  scattering and give a brief summary of the physics content of our model and determine the parameters which give an optimal description of  $pp$  data up to LHC. We shall then use the single-channel eikonal to calculate the inelastic non-diffractive  $pp$  cross-section and obtain the  $p - air$  production cross-section to compare with data.

## 2 Proton-proton total and inelastic non-diffractive cross-section

The eikonal function of the mini-jet model of [10, 11] is given by

$$\begin{aligned} 2\chi_I(b, s) &= n_{soft}^{pp}(b, s) + n_{jet}^{pp}(b, s) \\ &= A_{FF}(b)\sigma_{soft}^{pp}(s) + A_{BN}(p; b, s)\sigma_{jet}(PDF, p_{min}; s) \end{aligned} \quad (9)$$

where  $A_{FF}(b)$ , the impact parameter distribution in the non perturbative term, is obtained through a convolution of two proton form factors, whereas for the perturbative term, the distribution  $A_{BN}^{pp}(p; b, s)$ , multiplying the mini-jet contribution, is given by the Fourier transform of overall soft gluon re-summation, i.e. we have

$$A_{BN}^{pp}(p; b, s) = \frac{e^{-h(p;b,s)}}{\int d^2\mathbf{b} e^{-h(p;b,s)}} \quad (10)$$

where

$$h(p; b, s) = (\text{const}) \int_0^{q_{\max}} \frac{dk_t}{k_t} \alpha_s(k_t) \log \frac{2q_{\max}}{k_t} [1 - J_0(bk_t)] \quad (11)$$

and

$$\alpha_s(k_t) \simeq \left( \frac{k_t}{\Lambda_{QCD}} \right)^{-2p} \quad k_t \rightarrow 0 \quad (12)$$

We have discussed the distribution of Eq. (11) in many publications, its main characteristic is to include soft gluon re-summation down to  $k_t = 0$ , and regulate the infrared singularity so as correspond to a dressed gluon potential  $V(r) \sim r^{2p-1}$  for  $r \rightarrow \infty$ . The expression in Eq.(12) is an ansatz put forward in [13] inspired by the Richardson potential behaviour at large distances [20], and by Polyakov's argument [21] about linear Regge trajectories.

We have also shown an important consequence of an expression such as the above for  $\alpha_s(k_t \rightarrow 0)$  [22], namely that asymptotically the regularized and integrated soft gluon spectrum of Eq. (11) is seen to rise as

$$h(p; b, s) \rightarrow (b\bar{\Lambda})^{2p} \quad (13)$$

and thus the  $b$ - distribution exhibits a cut-off in  $b$ -space strongly dependent on the parameter  $p$ , i.e.

$$A_{BN} \rightarrow e^{-(b\bar{\Lambda})^{2p}} \quad b \rightarrow \infty \quad (14)$$

with  $\bar{\Lambda} \propto \Lambda_{QCD}$ . Since the mini jet cross-sections at low- $x$  are parametrized so as to rise as  $s^\epsilon$ , the behavior of Eq. (14) leads to a high energy behavior for the total cross-section given as

$$\sigma_{tot}^{pp} \sim \frac{2\pi}{(\bar{\Lambda})^2} [\epsilon \log s]^{1/p} \quad (15)$$

The parameter  $1/2 < p < 1$ : the lower limit so as to have a confining potential, the upper limit to insure convergence of the integral over the soft gluon spectrum of Eq. (11). An immediate consequence of this model is that the cross-section will never rise faster than  $[\log s]^2$ , the saturation of the Froissart limiting behavior being obtained for  $p = 1/2$ . Notice, that, in this model, the mini-jet contribution, just as in hard Pomeron models [23], rises as  $\sigma_{jet} \sim s^\epsilon$ , with  $\epsilon \sim 0.3-0.4$  depending on the low- $x$  parametrization of the PDF. However the strong cut-off in  $b$ -space brought in by the singular, but integrable, effective *quark – soft – gluon* coupling constant leads only up to a *(logarithmic)*<sup>2</sup> rise with energy. For more details, we refer the reader to [22].

The low energy term includes collisions with  $p_t \leq p_{tmin} \sim (1 \div 2) \text{ GeV}$ , and the cross-section  $\sigma_{soft}^{pp}(s)$  is not predicted by this model so far, thus we parametrize it here with a constant and one or more decreasing terms. The result is shown in Fig. 1.

The perturbative, mini-jet, part is defined with  $p_t^{parton} \geq p_{tmin}$  and is determined through a set of perturbative parameters for the jet cross-section, namely a choice of PDF and  $p_{tmin}$ . Since the soft gluon re-summation includes all order terms in soft gluon emission, as in previous publications we have used only LO densities. An important point of our approach is that we use the same, library distributed PDF, as used for jet physics. Previously

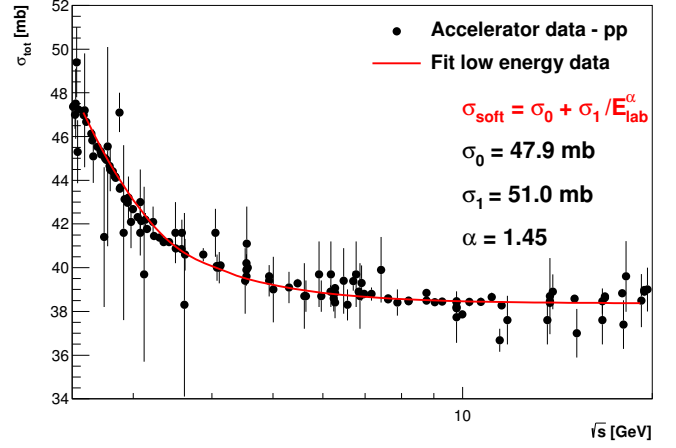


Figure 1. Low energy parametrization of  $pp$  total cross-section

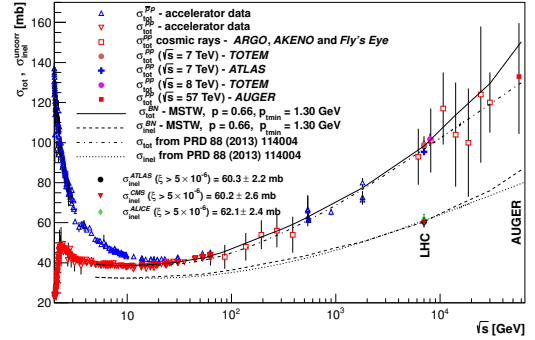


Figure 2. QCD mini-jet with soft gluon resummation model and  $pp$  total cross-section (full line) as described in the text. The determination of the optimal model parameters was done independently of the AUGER data. The dotted curve is from the mini-jet model of [18]. Accelerator data at LHC include TOTEM [29, 30] and ATLAS [31] measurements. The inelastic uncorrelated cross-section is given by the dashed curve and compared with central collisions results at LHC by ATLAS [32], CMS [33] and ALICE [34].

used PDFs were GRV [24–26], or MRST72 [27]. Both still give a good description of data up to LHC results, as shown here and in the next section. In Fig. 2 we show the results obtained through a more recent set of LO densities, MSTW [28], for both the total and the inelastic  $pp$  cross-sections. We notice here that the determination of the parameters, at low and high energy as well, was done without taking account the cosmic ray data points, namely the parameters were chosen so as to give good reproduction of ISR and LHC data only. The parameter  $p$ , whose value is explicitly given in this figure, is related to the amount of acollinearity induced by soft gluon emission, as discussed in [22]. Its value lies in the range  $0.6 \lesssim p \lesssim 0.8$  depending on the PDF used. For MSTW, we find that the parameter set  $\{p_{tmin} = 1.3 \text{ GeV}, p = 0.66\}$  best reproduces the  $pp$  cross-section up to LHC8.

We note the important result that the inelastic cross-section predicted by the parametrization of the total cross-section through a single-channel eikonal, reproduces very

well the LHC data for non-diffractive collisions by ATLAS [32], CMS [33] and ALICE [34]. Such agreement had already been highlighted in [7]. We shall return to comment on this point at the end of the paper.

In addition to the results from our model, Fig. 2 shows also the mini-jet result Ref. [18], where a different set of PDFs is used, and a different impact parameter distribution. The mini-jet contributions in these two applications of the mini-jet model are different, but both are based on a single-channel eikonal approach.

## 2.1 A comment on the model parameters

The present focus of our model is the parametrization of the high energy behavior described by QCD processes. To this aim, we need a set of PDFs, a lower cut-off dividing the perturbative and non-perturbative regions,  $p_{min}$ , and a parameter  $p$ , which we also referred to as *singularity* parameter. The higher this parameter, the more softened is the cross-section. Phenomenologically, its value is fixed in relation to the low- $x$  behavior of the densities. The parameter  $p$  thus appears to be unrelated to the perturbative expression for the QCD coupling constant  $\alpha_s(Q^2)$ . We however believe it to be of more fundamental interest, and have made the ansatz [35] that the actual expression to use in the integrand of Eq. (11) is

$$\alpha_s^{BN}(Q^2) = \frac{1}{\ln[1 + (\frac{Q^2}{\Lambda^2})^{b_0}]} \xrightarrow{Q^2 \gg \Lambda^2} \alpha_{AF}(Q^2) \quad (16)$$

where  $b_0 = (33 - 2N_f)/12\pi$  and the suffix *BN* is used to indicate its applicability into the infrared region (the one first explored in QED by Bloch and Nordsieck [36]), while coinciding with the usual one-loop asymptotic freedom expression at high  $Q^2$ . The above ansatz would imply that the infrared region description does not require introduction of an extra parameter  $p$ : the behavior from  $Q^2 = 0$  to  $Q^2 \rightarrow \infty$  is dictated only by the anomalous dimension factor. However, the present uncertainty about a fundamental calculation for the low- $x$  behavior of the parton densities, prevents a full use of Eq.(16). Suffice to say that our phenomenological values for  $p$  are in the same range of variability of the anomalous dimension factor  $b_0$ .

## 3 The production cross-section for $p - air$

With the low energy part parametrized as shown in Fig. 1, and the mini-jet part, we can calculate the inelastic  $pp$  cross-section and thus the production  $p - air$  cross-section. The result is shown in Fig. 3 where our model is compared with cosmic ray data [9, 37–43] and with two other mini-jet models, a recent one [18] and the first such application by Durand and Pi [15]. We notice that the old model is rather above the cosmic ray data point, as they are presently extracted. In this figure we have reduced the constants  $\sigma_{0,1}$  in the  $pp$  cross-section so as to comply with the surface/volume effect for the low transverse momentum collisions. Because of the uncertainty in this low energy region, the soft term in the  $pp$  cross-section has been

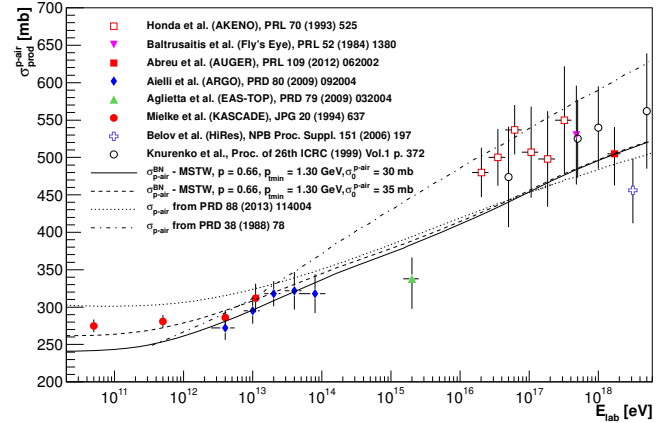


**Figure 3.**  $p - air$  production cross-section using MSTW2008 [28] parton densities in a single-channel eikonal mini-jet model with infrared gluon resummation. The two curves from the BN model (full and dashes) are obtained with a different low energy constant,  $\sigma_0$ . The results from the mini-jet model of [18] is given by the dotted curve. The dashed curve is the first mini-jet application of a mini-jet model for cosmic ray cross-section, from [15].

included openly as a constant. However, we have also considered the full low-energy parametrization of Figs. 1, 2, but in the energy range of Fig. 3 such low energy decreasing term makes no difference whatsoever.

To estimate the error of this procedure as well as check the stability of the model and its application to both  $pp$  and  $p - air$  cross-sections, we have done the following checks:

- after parametrizing the low energy part of  $pp$  data, the rise has been described through other available LO PDFs, namely MRST72 and GRV in addition to MSTW. For a given PDF set, the parameters  $p_{min}$  and  $p$  have been chosen to best reproduce LHC results for  $\sigma_{tot}^{pp}$  [29, 30].
- we have done an actual fit to both the low energy data and LHC (excluding cosmic rays extracted data), using GRV and MRST72, and with the free singularity parameter  $p$ .
- We have changed the nuclear density model, applying a Wood-Saxon potential, also applied, for instance, in [8] and [18].

The results of this exercise for different densities are shown in the two panels of Fig. 4, where the bands highlight the uncertainty related to the the low- $x$  behavior of the parton densities used for the mini jet calculation. As we are not so much interested in understanding right now the low energy part, the constant  $\sigma_0$  has simply been reduced adjusting it to the data. As expected, the contribution from the low energy part gets weaker and weaker for very high energies. The results are also shown in Table 1. In the table, the low energy part of the eikonal function,  $n_{soft}$ , is fitted to the low energy data alone, as in Fig. 1, whereas the QCD part  $n_{hard}$  is chosen so as to best describe the  $pp$  accelerator data. As for the other check, non reproduced in this table, namely fitting at the same

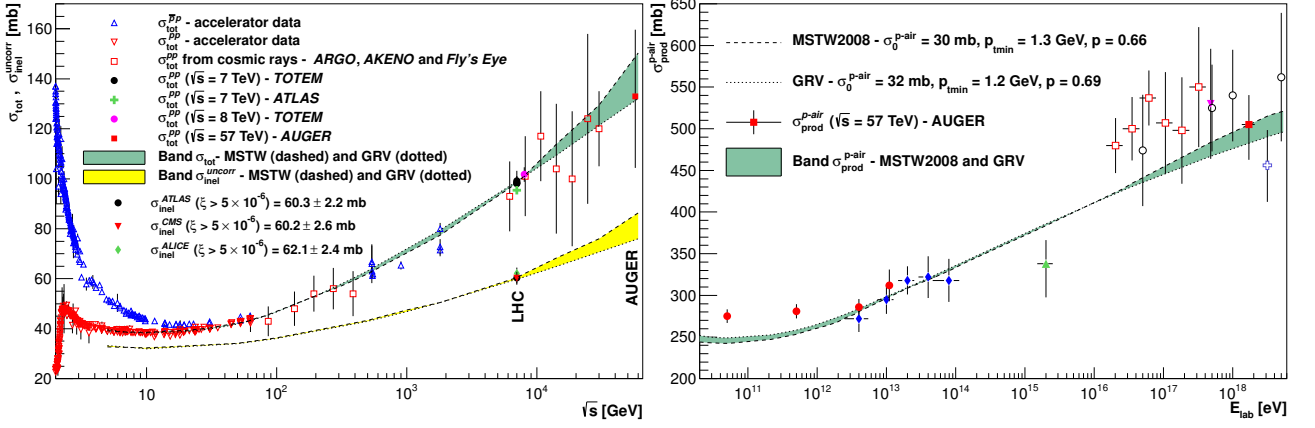


**Figure 4.** Left panel: total and uncorrelated inelastic  $pp$  cross-sections for different PDF sets. Right panel: the production  $p - air$  cross-section following the results from the left panel. The green and yellow bands indicate the uncertainty related to the low- $x$  behavior of the PDF used. Symbols for  $p - air$  data as in Fig. 3.

**Table 1.** Total and inelastic uncorrelated  $pp$  cross-sections (second and third column). Fourth column is the uncorrelated inelastic  $pp$  cross-section for input to the Glauber formula for  $\sigma^{p-air}$ , with low energy part reduced for nuclear area/volume effect. Last column shows the resulting  $p - air$  cross-section. Different parameter sets are as indicated.

Parameter set : GRV, $p_{min} = 1.2 GeV, p=0.69$				
$\sqrt{s} (GeV)$	$\sigma_{tot}^{pp}$ with $\sigma_0 = 48 mb$	$\sigma_{inel}^{pp-uncorr}$ with $\sigma_0 = 48 mb$	$\sigma_{inel}^{pp-uncorr}$ with $\sigma_0 = 32 mb$	$\sigma_{prod}^{p-air}$ $\sigma_0 = 32 mb$
5	39.9	33.2	24.9	255.8
10	38.2	32.0	24.0	248.9
50	41.9	34.0	26.7	268.7
100	46.7	36.1	29.7	288.6
500	63.2	43.0	38.6	340.9
1000	71.7	46.9	43.1	364.1
1800	79.5	50.5	47.2	383.5
7000	98.9	59.8	57.4	426.1
8000	100.9	60.7	58.4	430.0
14000	109.3	64.8	62.8	445.9
30000	121.3	70.7	69.0	467.0
60000	132.0	76.0	74.6	484.3
Parameter set : MRST72, $p_{min} = 1.25 GeV, p=0.62$				
$\sqrt{s} (GeV)$	$\sigma_{tot}^{pp}$ with $\sigma_0 = 48 mb$	$\sigma_{inel}^{pp-uncorr}$ with $\sigma_0 = 48 mb$	$\sigma_{inel}^{pp-uncorr}$ with $\sigma_0 = 32 mb$	$\sigma_{prod}^{p-air}$ $\sigma_0 = 32 mb$
5	39.9	33.2	24.9	255.8
10	38.3	32.0	24.0	249.1
50	43.1	34.6	27.6	274.5
100	48.4	36.9	30.8	295.8
500	63.8	43.7	39.3	344.6
1000	71.3	47.1	43.3	365.1
1800	78.1	50.3	46.9	382.3
7000	98.2	60.4	58.0	428.3
8000	100.7	61.7	59.4	433.6
14000	112.2	67.7	65.7	456.2
30000	129.1	76.5	75.0	485.7
60000	144.2	84.4	83.3	509.1
Parameter set : MSTW, $p_{min} = 1.3 GeV, p=0.66$				
$\sqrt{s} (GeV)$	$\sigma_{tot}^{pp}$ with $\sigma_0 = 47.9 mb$	$\sigma_{inel}^{pp-uncorr}$ with $\sigma_0 = 47.9 mb$	$\sigma_{inel}^{pp-uncorr}$ with $\sigma_0 = 30 mb$	$\sigma_{prod}^{p-air}$ $\sigma_0 = 30 mb$
5	39.21	32.7	23.7	246.8
10	38.60	32.3	23.1	242.6
50	42.2	34.2	25.9	263.4
100	46.9	36.4	29.2	285.5
500	62.0	43.3	38.1	338.6
1000	71.0	47.5	43.1	364.4
1800	77.5	50.5	46.6	381.2
7000	98.3	60.5	57.8	428.0
8000	101.3	62.0	59.4	434.0
14000	113.7	68.2	66.1	457.7
30000	129.4	76.0	74.3	483.8
60000	150.3	86.3	85.1	514.3

time both the low and the high energy accelerator data in order to determine the best  $p$ -value, for a given choice of PDF and  $p_{min}$ , we have found the result to be consistent with above, for  $p \approx 0.6$  for MRST72 densities and  $p_{min} \approx (1.3 \div 1.4) GeV$ . Using the Wood-Saxon potential slightly lowers the curves for  $p - air$  with respect to

the standard nuclear potential of Eq. (3). Before concluding, we would like to return to an important physics point, namely that the experimentally measured  $\sigma_{p-air}^{prod}$  differs from the total  $\sigma_{p-air}^{tot}$  through the exclusion of elastic  $\sigma_{p-air}^{el}$  as well as quasi-elastic  $\sigma_{p-air}^{q-el}$ . An example of  $\sigma_{p-air}^{q-el}$  is given by processes such as  $p + N \rightarrow p^* + N$ .

In general, one has to carefully examine the contribution that the measured cosmic ray particle production cross-section receives from (single as well as double) diffractive processes. It is possible that at the very high energies reached by present day cosmic ray experiments, and as proposed in [3], diffraction needs not to be included. This acquires a particular significance (and endows a certain simplicity) to (single-channel) mini-jet models when applied to an analysis of cosmic ray cross-sections. As we have discussed, the inelastic cross-section in such models only includes uncorrelated process, and does not include the diffractive part. Our present proposal is that the single-channel approach is thus best suited for calculations of the production  $p - air$  cross-section from cosmic ray measurements at ultra high energies. For this purpose, we have employed parameters (such as  $p$ ) suitable for describing the total cross-section well and by default giving us the inelastic part devoid of diffraction. A posteriori, such a description seems to work quite well.

The most remarkable result that we find is that we reproduce very well the AUGER point, in addition to have a reasonably good description of all the more recent cosmic ray measurements. At the AUGER point, our result agrees with predictions of recent (much more complex) MC interaction codes, such as QGSJET01c [44]. We notice once more that our result is obtained in the context of a single-channel eikonal formalism and a good description of the accelerator data for  $pp$  total cross-section, to which we arrived without attempting to reproduce the extracted  $pp$  value at cosmic ray data energies.

## 4 Concluding remarks

In this contribution, we have seen that the Glauber formula in conjunction with an inelastic  $pp$  cross-section obtained through a single-channel eikonal formalism provides a very good description of the cosmic ray extracted ( $p - air$ ) cross-section. Thus, we might ask, whether a single-channel eikonal expression adequately representing the  $pp$  total cross-section is also sufficient to describe high energy elastic scattering. Obviously not. However, it is fair to say that the momentum transfer ( $t$ )-dependence of the elastic differential cross-section from the forward ( $t = 0$ ) up to after the dip still escapes a fundamental QCD explanation. For this, and thus for the diffractive part of the cross-section, a multi channel formalism [45–47] is still required. However, it is our ansatz that a viable multi-channel formalism must be geared to reproduce the results from a single term at the optical point (that is at  $t = 0$ ).

For the present, we may reiterate that a good single-channel eikonal representation for the total cross-section should be sufficient to describe the cosmic ray  $p - air$  production cross-section data and conversely, that models which reproduce  $\sigma_{production}^{p-air}$  can be trusted to extrapolate correctly  $\sigma_{inel-non-diffractive}^{pp}$ , and thus the total  $\sigma_{tot}^{pp}$  in a single-channel eikonal model. However, very high energy predictions are affected by an uncertainty related to the low- $x$  behavior of the PDFs used in the phenomenological calculation of the mini-jet cross-sections. It may thus be very important to include the forthcoming LHC data at  $\sqrt{s} > 10 TeV$  to reduce such uncertainty and hopefully be able to extract information on  $\sigma_{tot/inel}^{pp}$  from the even higher energy cosmic ray measurements to be expected from cosmic rays.

## Acknowledgments

A.G. acknowledges partial support by Junta de Andalucia (FQM 6552, FQM 101). D.A.F. acknowledges the São Paulo Research Foundation (FAPESP) and the Coordination for the Improvement of Higher Education Personnel (CAPES) for financial support (contract: 2014/00337-8). O.S. acknowledges partial support from funds of Foundation of Polish Science grant POMOST/2013-7/12, that is co-financed from European Union, Regional Development Fund.

## References

- [1] R. J. Glauber, *High energy collision theory*, Interscience Publishers Inc., New York, 1959. In *Lectures in Theoretical Physics*, Vol. I, Boulder 1958.
- [2] V. Gribov, *Sov. Phys. JETP* **29**, 483 (1969).
- [3] M. M. Block, *Phys. Rept.* **436**, 71 (2006); arXiv:hep-ph/0606215.
- [4] B.Z. Kopeliovich, *Phys. Rev.* **C68**, 044906 (2003).
- [5] L. Anchordoqui, M. T. Dova, A. G. Mariuzzi, T. McCauley, T. C. Paul, *et al.*, *Annals Phys.* **314**, (145-207) (2004); arXiv:hep-ph/0407020.
- [6] G. Antchev, *et al.* (TOTEM Collaboration), *Europhys.Lett.* **101**, 21003 (2013).
- [7] A. Achilli, R. M. Godbole, A. Grau, G. Pancheri, Y. N. Srivastava, O. Shekhovtsova, *Phys. Rev.* **D84**, 094009 (2011); arXiv:1102.1949.
- [8] E. Gotsman, E. Levin, U. Maor, *Phys. Rev.* **D88**, 114027(2013); arXiv:1308.6660.
- [9] P. Abreu, *et al.* (Pierre Auger Collaboration), *Phys. Rev. Lett.* **109**, 062002 (2012); arXiv:1208.1520.
- [10] R. M. Godbole, A. Grau, G. Pancheri, Y. N. Srivastava, *Phys. Rev.* **D72**, 076001(2005); arXiv:hep-ph/0408355.
- [11] A. Grau, G. Pancheri, Y. Srivastava, *Phys. Rev.* **D60**, 114020 (1999); arXiv:hep-ph/9905228.
- [12] G. Pancheri, Y. N. Srivastava, *Phys. Lett.* **B182**, 199-207 (1986).
- [13] A. Corsetti, A. Grau, G. Pancheri, Y. N. Srivastava, *Phys. Lett.* **B382**, 282 (1996); arXiv:hep-ph/9605314.
- [14] T. K. Gaisser, F. Halzen, *Phys. Rev. Lett.* **54**, 1754 (1985).
- [15] L. Durand, H. Pi, *Phys. Rev.* **D38**, 78 (1988).
- [16] L. Durand, H. Pi, *Phys. Rev.* **D40**, 1436 (1989).
- [17] M. M. Block, F. Halzen, G. Pancheri, T. Stanev (2000). arXiv:hep-ph/0003226.
- [18] A. Giannini, F. Duraes, *Phys. Rev.* **D88**, 114004 (2013); arXiv:1302.3765.
- [19] R. J. Glauber, G. Matthiae, *Nucl. Phys.* **B21**, 135 (1970).
- [20] J. L. Richardson, *Phys. Lett.* **82B** 272 (1979).
- [21] A.M. Polyakov, *JETP Lett.* **20**, 194 (1974).
- [22] A. Grau, R. M. Godbole, G. Pancheri, Y. N. Srivastava, *Phys. Lett.* **B682**, 55 (2009); arXiv:0908.1426.
- [23] M. G. Ryskin, A. D. Martin, V. A. Khoze, *Eur. Phys. J.* **C71**, 1617 (2011); arXiv:1102.2844.
- [24] M. Gluck, E. Reya, A. Vogt, *Z. Phys.* **C53**, 127 (1992).
- [25] M. Gluck, E. Reya, A. Vogt, *Z. Phys.* **C67**, 433 (1995).
- [26] M. Gluck, E. Reya, A. Vogt, *Eur. Phys. J.* **C5**, 461 (1998); arXiv:hep-ph/9806404.
- [27] A. D. Martin, R. G. Roberts, W. J. Stirling, R. S. Thorne, *Eur. Phys. J.* **C4**, 463 (1998); arXiv:hep-ph/9803445.
- [28] A. Martin, W. Stirling, R. Thorne, G. Watt, *Eur. Phys. J.* **C63**, 189 (2009); arXiv:0901.0002.
- [29] G. Antchev *et al.* (TOTEM Collaboration), *Phys. Rev. Lett.* **111**, 1, 012001(2013).
- [30] G. Antchev *et al.* (TOTEM Collaboration), *Europhys. Lett.* **101**, 21004 (2013).
- [31] Georges Aad *et al.* (ATLAS Collaboration), *Nucl.Phys.* **B889** 486-548 (2014).
- [32] G. Aad, *et al.* (ATLAS Collaboration), *Nature Commun.* **2**, 463 (2011); arXiv:1104.0326; *Nucl. Phys.* **B889**, 486 (2014)
- [33] S. Chatrchyan, *et al.* (CMS Collaboration), *Phys. Lett.* **B722**, 5 (2013): arXiv:1210.6718.

- [34] B. Abelev, *et al.* (ALICE Collaboration), *Eur. Phys. J.* **C73**, 2456 (2013); arXiv:1208.4968.
- [35] G. Pancheri, D. A. Fagundes, A. Grau, O. Shekhovtsova, Y. N. Srivastava (2014). arXiv:1403.8050.
- [36] F. Bloch, A. Nordsieck, *Phys. Rev.* **52**, 54 (1937).
- [37] R. Baltrusaitis, G. Cassiday, J. Elbert, P. Gerhardy, S. Ko, *et al.*, *Phys. Rev. Lett.* **52**, 1380 (1984)
- [38] M. Honda, M. Nagano, S. Tonwar, K. Kasahara, T. Hara, *et al.*, *Phys. Rev. Lett.* **70**, 525 (1993).
- [39] H. Mielke, M. Foeller, J. Engler, J. Knapp, *J. Phys. G* **20**, 637 (1994).
- [40] S. Knurenko, V. Sleptsova, I. Sleptsov, N. Kalmykov, S. Ostapchenko, *Salt Lake City, Proc. of 26th ICRC* **1**, 372 (1999).
- [41] K. Belov (HiRes Collaboration), *Nucl. Phys. Proc. Suppl.* **151**, 197 (2006).
- [42] M. Aglietta, B. Alessandro, P. Antonioli, F. Arneodo, L. Bergamasco, *et al.*, *Phys. Rev.* **D79**, 032004 (2009).
- [43] G. Aielli, *et al.* (ARGO-YBJ Collaboration), *Phys. Rev.* **D80**, 092004 (2009).
- [44] S.P. Knurenko and A. Sabourov, *EPJ Web Conf.* **53** 07006 (2013).
- [45] V. A. Khoze, A. D. Martin, M. Ryskin, *Eur. Phys. J.* **C18**, 167 (2000); arXiv:hep-ph/0007359.
- [46] P. Lipari, M. Lusignoli, *Phys. Rev.* **D80** (2009) 074014 (2009); arXiv:0908.0495.
- [47] E. Gotsman, E. Levin, U. Maor, *Phys. Rev.* **D85** (2012) 094007 (2012); arXiv:1203.2419.